Referee # 3:

I suggest adding a comment on that salinity and TA in seawater did not have the same concentrations before the experiment (t=0) and after (=end) the experiment due to remaining sea ice in the pool. That is what I mean with "closing the TA budget" (perhaps wrong wording). TA should be the same in the seawater before and after finishing the experiment, if all ice melted (and taking into account the sampled ice TA). For clarification, please just add a comment in the method section or when introducing Table 1 or Figure 2.

→We have changed the caption for table 1 to:
"Note that seawater salinity and $TA_{(sw)}$ do not reach the initial seawater values as sea ice was still present at the end of the experiment."
We also added a comment on line 229 in the introduction of the TA and TCO_2 measurements in the pool that reads "As the experiment stopped before the ice was completely melted in the tank, both the seawater salinity and $TA_{(sw)}$ do not reach their initial values at the end of the experiment (Table 1, Fig 2 and 3)."

Lines 510-513, after comment on the study by Fransson et al 2013 "....release of brine decreased Ωaragonite by 0.8 ......related to CO2 enrichment of brine". I suggest adding (for consistency): "Conversely, during ice melt, Ωaragonite increased by 1.4 between March and May, likely due to both CaCO3 dissolution and primary production. This contrasts...."

→We followed the suggestion. Thanks.

Line 517, after .....DOE (1994). "This shows the complexity of ikaite and its impact on the carbonate system and Ω in the underlying water."

→We followed the suggestion. Thanks.

Line 528. Add "may" before "therefore" so that the sentence reads "....impede the effect of ikaite rejection and may therefore lower Ωaragonite.

→We followed the suggestion. Thanks.

Table 2. Please check the significant numbers of decimals and values for all the parameters. Are two decimals significant regarding the accuracy in the measurements and calculations? I think that one or no decimal is more accurate. This is valid also for Figure 6 linear regression equations and R2.
Table 2. What parameter is in the first column (and unit?)? Date/time in decimals?

→The rule of significant numbers specifies that we should use the number of significant figures in the factor with the least significant figures. In our case, the least amount of significant figures is 4 (sea ice and seawater volume). Therefore, all data presented in table 2 has a maximum of 4 significant numbers. Data from table 2 are also rounded to the number of significant figures in the factor with the least significant figures (here again, 4). Which is why, for small values, we

keep 2 decimals. The first column is the Day-of-year (DOY). We've added this information in the table.

Suggested additional reference Lyakhin (1970): show evidence that sea ice can release solid CaCO3 to the underlying water
Reference:
Lyakhin, Y. I. (1970), Saturation of water of the Sea of Okhotsk with calcium carbonate, Oceanology, 10, 789–795.
→ Thanks for the reference, however I don't have the reference and I have a hard time finding it.

Referee # 4:
The paper analyses a three week mesocosm study performed at the outdoor sea ice research facility SERF in Winnipeg with respect to the transfer of ikaite crystals to the underlying water during sea ice growth and melt, and it;'s effect on the water and ice carbon budget. The facility allows for a constrained environment which allows to analyze the full "ocean" budget, with out the uncertainty of horizontal and vertical processes in a deep ocean.

The study seems a reasonable set up and analyses performed adequately. The results provide some important additions to our understanding of the role of ikaite precipitation and dissolution during sea ice growth and melt processes.

I recommend publication with minor revisions.

Requested revisions are mostly minor clarifications with a few concerns with respect to the suitability of the set up for the analysis of specific processes. My main question is with respect to the melting procedure, i.e. does melting initiated from an underwater source provide the adequate representation for sea ice melting usually initiated by atmospheric warming and incident shortwave. This is particularly relevant when discussing release of ikaite crystals through melted channels at the bottom of the sea ice versus exchange of CO2 at the surface.

→SERF experiments are of course inherently constrained by the facility's infrastructure; it is not possible to simulate sea ice melt during January from the top as might occur in the Arctic. However, the bottom sea ice melt prescribed in this experiment was as representative as possible of the natural environment. For example, (i) the case of incomplete sea ice cover with substantial spring/summer incident radiation heating the surface ocean (e.g. Babb et al., 2016), or (ii) complete sea ice cover in the presence of a substantial ocean heat flux (REF). The heat was turned on in the pool while the atmospheric temperature was increasing (see figure 2). Changes observed in the ice cover (temperature, salinity, opening of the brine channels) occur in the same way as in polar regions under similar forcing.
Specifically addressing the reviewer's comment above regarding "discussing release of ikaite crystals through melted channels at the bottom of sea ice versus exchange of CO_2 at the surface", observation of spring/summer sea ice temperature profiles as the ice warms have long indicated that the middle the sea ice volume stays the coldest the longest; this cold middle area inhibits connectivity between the warming surface ice layer and the relatively warm bottom ice layer bathed in seawater warmed by incident solar radiation. For example, Babb et al., (2016) show 198 cm of bottom melt vs. 135 cm of surface melt as a multiyear sea ice floe (523cm winter thickness) warmed with a continuously c-shaped temperature profile.
Babb, D.G. and others, 2016, Physical processes contributing to an ice free Beaufort Sea during September 2012, Journal of Geophysical Research Oceans, 121, 267-283, doi: 10.1002/2015JC010756.

Minor comments:

Abstract

The first 1-3 sentences seem a bit disconnected and I am feeling I am missing a sentence on what ikaite is about.
→ The first 3 sentences were already changed in the most recent version. The reviewer has read and reviewed a previous version of the manuscript.

sentence 1 could be
→I don't understand what the reviewer means by this comment.
L14 rm "from open water"
→This sentence has changed since the version on which the reviewer commented.

L19 up to => therefrom , then rm :of the ikaite...within sea ice"
→ This sentence has changed since the version on which the reviewer commented.

Main text:
L29 released to the atmosphere - from where?
→The sentence refers to anthropogenic carbon, the release of carbon due to human activities.

L50 rejected from sea ice - clarify direction (where to)
→ We've added "...to the underlying seawater"

L67/68 fluxes are....incorporated into water masses ....or below sea ice – something is wrong here, please clarify sentence
→The sentence was already edited as a result of the previous round of review.

L70 Are you referring to the shrinking of the brine channels due to freezing ? If so please clarify
→We prefer to leave this sentence as it is.

L72-74 would move the "internal ice melt" forward , since that is what increases the ibrine volume, correct?
→ The sentence to which the reviewer is referring currently states that internal melting dilutes brine resulting in decreased brine salinity. This of course would increase the brine volume, but the important point here is decreased brine salinity as it relates to decreased TA and TCO_2 leading to lower pCO_2. So, we prefer to leave the sentence as it stands.

L75 Eq 3 – should this be Equ 1?
→This was corrected in the previous round of revisions.

L86 of the different processes
→We've made the suggested change.

L90 the addition "from open water" makes the sentence a bit convoluted. I think it would be sufficient to clarify once at the beginning that the experiment starts

with open water, then only write " from initial sea ice formation to melt" (This occurs several times in the manuscript)
→We followed the suggestion, thanks.

L95 suggest to rm "major changes in"
→We deleted "major" from the sentence.

L104 formulated => formed ???
→This text was changed to "made by" in the previous round of reviews.

L106ff How realistic is it to have an under water heat source versus an atmospheric heat source, particularly in terms of melting the ice structure and opening of brine channels from top or bottom, allowing fluxes out of the ice ???
→We have endeavored to address this comment on the first page of this document when the question of heating from below was first raised by the reviewer.

L113 How well mixed is the underlying water – is 1.3m a representative depth?
→The 1.3m was chosen because it is half of the seawater depth in the pool (cf. line 109 in the newer version). A discussion on how well mixed the pool can be found lines 219-222 of the most recent version of the manuscript.

L244 rm Therefore (previous sentence is not the cause of this)
→The sentence was changed in the previous round of revision of the manuscript.

L 260 expected : expected based on what? (does that refer to no ikaite interaction?)
→Expected based on the fact that TA and TCO_2 are conservative with salinity (cf the beginning of the sentence.) The sentence was changed in the most recent round of revisions prior to this review (line 299).

L267 throughout the ice
→ The sentence was changed in the most recent round of revisions prior to this review.

section 5.2.1 Suggest to define some dTA for the difference between TA(ice)* and TA(ice), this might make the text clearer.
→We prefer to keep the text as it is now.

L279 black dots =diamonds
→We made the suggested change.

L280 .. highly variable (isn't that something that would be expected, ie. Concentration needs to become high enough for crystallization, but once it is precipitated the concentration needs to be build up again before more crystallization can happen??? - not sure, I am not a chemist...)
→ It is expected as this is something we observed by direct observation in the manuscript of Rysgaard et al (2014) (during the same SERF experiment). By

variable we mainly suggest that ikaite can precipitate-dissolve during the same experiment, based on the ice temperature, as suggested by Rysgaard et al (2014).

L282 I can't see this in the Figure (7a??) please clarify. If differences are minor a zoom in and clarification might help.
→These differences are displayed on Figure 7c, as mentioned in the text (in both old and new version of the manuscript).

L290-309 This section would profit from some streamlining, as is the message is confusing
e.g. L299 you talk about underestimation while the figure shows mostly overestimation till Jan 17. While this is addressed later it doesn't make sense where it is stated.
L301-303 could ikaite also be redissolved with sea water infiltration?
L307-308 clarify that the message is precip is not only reduced but actual dissolution occurs
L309 can you discern this from the water column? If so state this and refer to section where this is discussed
→This whole section (5.2.1. Sea ice) has been changed as a result of the previous round of revision; it's now lines 316-358 in the newest version.

Section 5.22 could the export towards the underlying sea water be intensified by the melting from the bottom? (Since it already starts before the melting is turned on, it might not be the case, but it might be good to discuss.
→Here as well, we substantially changed section 5.3 "Ikaite export from the ice to the water column" as a result of the previous round of revision. The reviewers' concern above is addressed in the newest version of the paper.

L320 one-month long – Isn't the experiment 17 days only or is this another experiment?
→The text has been changed according to previous reviewer asking the same thing.

L 326 started => starts
→ Thank for the correction.

L 320-349 again, this starts to become confusing, any streamlining would help
→ We substantially changed this text as a result of the previous round of revision. The reviewers' concern above is addressed in the newest version of the paper.
L344 delay of reaction ??
→ 1 day delay. The text changed in the newer version of the manuscript.

L358 Please clarify if you were actually measuring ikaite or derived it.
→ We substantially changed this text as a result of the previous round of revision. The reviewers' concern above is addressed in the newest version of the paper.

L367 rm contain

→ The sentence was changed in the most recent round of revisions prior to this review.

5.4 This title is strange, I suggest to put the " attempt of a CO2 budget in a separate section (from line 400 and maybe frame it as an error or uncertainty analysis...)
→ We have changed the title of this section; it now reads "Air-ice-seawater exchange of inorganic carbon".

L399 Are you generating this kind of turbulence in the tank?
→4 pumps were installed at the bottom of the pool to inducing a consistent current. This is explained in the new version of the manuscript, line 121, in the method section.

L424 Suggest: As a result several area => Several areas
→Already corrected, thanks.

L427 the annual
→Already corrected, thanks.

L428 saturation state
→Thanks for the correction.

L440 suggest using "alleviate" instead of "hamper"
→Thanks for the correction.

L448 month-long – 17 day?
→Already corrected, thanks.

L449 rm "from open water"
→We've removed "open water".

L450 suggest "direct CO2 exchange" to clarify this is released from the ice to the atmosphere
→During this experiment, we measured released of CO_2 from the ice to the atmosphere and uptake of atmospheric CO_2. Therefore we will keep the sentence at it is now.

L452 estimation => estimates; rm here
→The text changed in the new version of the manuscript, thanks.

L455 were missing ???? had been removed?
→The text changed in the new version of the manuscript, thanks.

L470 responsible formation
→The text changed in the new version of the manuscript, thanks.

Figure 2 use consistent ABCD, abcd in caption and figure
→This has been corrected in the new version, thanks.

Panel d indicate blue and green, What is the black line in panel d, also the different symbols are not discernible
→This has been corrected in the new version, thanks.

caption last line: profile => profiles
→Thanks for the correction.

Fig 3 caption clarify what is indicated with * (E.g. add in brackets after "variation of salinity observed" (**).
→This has been corrected in the new version, thanks.

Fig. 6 what are the green and blue lines
→This has been corrected in the new version, thanks.

1   **Estimates of ikaite export from sea ice to the underlying seawater in a sea**

2   **ice-seawater mesocosm**

3   Geilfus N.-X.[1,2], Galley R. J.[1], Else B. G. T.[3], Campbell K.[1], Papakyriakou T.[1], Crabeck O.[1], Lemes M.[1], Delille

4   B.[4], Rysgaard S.[1,2,5]

5   [1] Centre for Earth Observation Science, Department of Environment and Geography, University of Manitoba,
6   Winnipeg, Canada
7   [2] Arctic Research Centre, Aarhus University, Aarhus, Denmark
8   [3] Department of Geography, University of Calgary, Calgary, Canada
9   [4] Unité d'Océanographie Chimique, Université de Liège, Liège, Belgium
10   [5] Greenland Climate Research Centre, Greenland Institute of Natural Resources, Nuuk, Greenland

11   **1. Abstract**

12   The precipitation of ikaite and its fate within sea ice is still poorly understood. We quantify temporal

13   inorganic carbon dynamics in sea ice from initial formation to its melt in a sea ice-seawater mesocosm

14   pool from 11 to 29 January 2013. Based on measurements of total alkalinity (TA) and total dissolved

15   inorganic carbon ($T\mathrm{CO_2}$), the main processes affecting inorganic carbon dynamics within sea ice were

16   ikaite precipitation and $\mathrm{CO_2}$ exchange with the atmosphere. In the underlying seawater, the dissolution of

17   ikaite was the main process affecting inorganic carbon dynamics. Sea ice acted as an active layer,

18   releasing $\mathrm{CO_2}$ to the atmosphere during the growth phase, taking up $\mathrm{CO_2}$ as it melted and exporting both

19   ikaite and $T\mathrm{CO_2}$ into the underlying seawater during the whole experiment. Ikaite precipitation of up to

20   167 µmol kg^{-1} within sea ice was estimated while its export and dissolution into the underlying seawater

21   was responsible for a TA increase of 64 to 66 µmol kg^{-1} in the water column. The export of $T\mathrm{CO_2}$ from

22   sea ice to the water column increased the underlying seawater $T\mathrm{CO_2}$ by 43.5 µmol kg^{-1}, suggesting that

23   almost all of the $T\mathrm{CO_2}$ that left the sea ice was exported to the underlying seawater. The export of ikaite

24   from the ice to the underlying seawater was associated with brine rejection during sea ice growth,

25   increased vertical connectivity in sea ice due to the upward percolation of seawater, and meltwater

26   flushing during sea ice melt. Based on the change in TA in the water column around the onset of sea ice

27   melt, more than half of the total ikaite precipitated in the ice during sea ice growth was still contained in

28   the ice when the sea ice began to melt. Ikaite crystal dissolution in the water column kept the seawater

29      $p\mathrm{CO_2}$ undersaturated with respect to the atmosphere in spite of increased salinity, TA, and $T\mathrm{CO_2}$

30   associated with sea ice growth. Results indicate that ikaite export from sea ice and its dissolution in the

31 underlying seawater can potentially hamper the effect of oceanic acidification on the aragonite saturation

32 state ($\Omega_{aragonite}$) in fall and winter in ice-covered areas, at the time when $\Omega_{aragonite}$ is smallest.

33 **2. Introduction**

34 Currently, each year, 7 Pg of anthropogenic carbon are released to the atmosphere, 29% of which is

35 estimated to be taken up by the Oceans through physical, chemical and biological processes (Sabine et al.,

36 2004). The Arctic Ocean are taking up -66 to -199 Tg C year^{-1}, contributing 5-14% to the global ocean

37 CO_2 uptake (Bates and Mathis, 2009), primarily through primary production and surface cooling

38 (MacGilchrist et al., 2014). However, polar ocean CO_2 uptake estimates consider sea ice as an

39 impermeable barrier, ignoring the potential role of ice-covered areas on gas exchange between the ocean

40 and atmosphere. Recent studies have shown that sea ice covered areas participate in the variable

41 sequestration of atmospheric CO_2 into the mixed layer below the ice (e.g. Papakyriakou and Miller 2011;

42 Geilfus et al., 2012; Nomura et al., 2013; Delille et al., 2014; Geilfus et al., 2014; 2015). Studies are

43 required to elucidate the processes responsible as well as their magnitudes both temporally and spatially.

44 The carbonate chemistry in sea ice and brine is spatially and temporally variable, which leads to

45 complex CO_2 dynamics with the potential to affect the air-sea CO_2 flux (Parmentier et al., 2013). Release

46 of CO_2 from sea ice to the atmosphere has been reported during sea ice formation from open water

47 (Geilfus et al., 2013a) and in winter (Miller et al., 2011; Fransson et al., 2013) while uptake of CO_2 by sea

48 ice from the atmosphere has been reported after sea ice melt onset (e.g. Semiletov et al., 2004; Nomura et

49 al., 2010; Geilfus et al., 2012; Nomura et al., 2013; Fransson et al., 2013; Geilfus et al., 2014; 2015). In

50 combination, these works suggest that the temporal cycle of sea ice formation and melt affects

51 atmospheric CO_2 uptake by the ocean in variable ways. Sea ice may also act as an important control on

52 the partial pressure of CO_2 (pCO_2) in the sea surface through a sea ice pump (Rysgaard et al., 2007).

53 During the earliest stages of sea ice formation, a small fraction of CO_2-supersaturated brine is expelled

54 upward onto the ice surface promoting a release of CO_2 to the atmosphere (Geilfus et al., 2013a). As sea

55 ice forms and grows thicker, salts are partly rejected from the sea ice to the underlying seawater and

56 partly trapped within the sea ice structure, concentrated in brine pockets, tubes and channels. As a result,

57 the concentration of dissolved salts, including inorganic carbon, increase within the brine and promote the

58 precipitation of calcium carbonate crystals such as ikaite ($CaCO_3 \bullet 6H_2O$) (Marion 2001). These crystals

59 have been reported in both natural (Dieckmann et al., 2008; Nomura et al., 2013, Søgaard et al., 2013)

60 and experimental sea ice (Geilfus et al., 2013b; Rysgaard et al., 2014) and have been suggested to be a

61 key component of the carbonate system (Rysgaard et al., 2007; Fransson et al., 2013; Delille et al., 2014).

62 During ikaite precipitation within sea ice, TA in brine is reduced by 2 moles due to the reduction of

63 bicarbonate (HCO$_3^-$) while TCO$_2$ in brine is only reduced by 1 mole (equation 1 to 3).

64 $$Ca^{2+} + 2HCO_3^- + 5H_2O \rightleftharpoons CaCO_3 \cdot 6H_2O + CO_2 \tag{1}$$
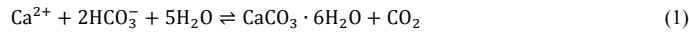
65 $$T\text{CO}_2 = [HCO_3^-] + [CO_3^{2-}] + [CO_2] \tag{2}$$

66 $$TA = [HCO_3^-] + 2[CO_3^{2-}] + [B(OH)_4^-] + [OH^-] - [H^+] \tag{3}$$

67 The specific conditions leading to ikaite precipitation as well as the fate of these precipitates in sea ice are

68 still not fully understood. Ikaite crystals may remain within the ice structure while the CO$_2$ formed during

69 their precipitation is likely rejected with dense brine to the underlying seawater and sequestered below the

70 mixed layer. During sea ice melt, the dissolution of these crystals triggered by increased ice temperatures

71 and decreased bulk ice salinity will consume CO$_2$ and drive a CO$_2$ uptake from the atmosphere to the ice.

72 Such mechanism could be an effective sea ice pump of atmospheric CO$_2$ (Delille et al., 2014). In

73 addition, ikaite stored in the ice matrix could become a source of TA to the near-surface ocean upon its

74 subsequent dissolution during sea ice melt (Rysgaard et al., 2007; 2009).

75 The main air-sea fluxes of CO$_2$ and TCO$_2$ are driven by brine rejection to the underlying seawater and

76 its contribution to intermediate and deep-water formation (Semiletov et al., 2004; Rysgaard et al., 2007,

77 2009; Fransson et al., 2013) or below sea ice in ice tank studies (e.g. Killawee et al., 1998 and

78 Papadimitriou et al., 2004). As sea ice thickens, reduced near-surface ice temperatures result in reduced

79 brine volume content, increased brine salinity and increased solute concentration in the brine. In the

80 spring-summer, as the ice temperature increases, sea ice brine volume increases and sea ice becomes

81 vertically permeable to liquid (Golden et al., 2007), enhancing the potential CO$_2$ exchange between the

82 atmosphere, sea ice and ocean. Eventually internal ice melt promotes brine dilution, which decreases

83 brine salinity, TA, TCO$_2$, and leads to lower pCO$_2$ in the brine. In addition, the dissolution of ikaite

84 decreases brine pCO$_2$ (Eq. 1) (Geilfus et al., 2012; 2015). These conditions all favour sea ice as a sink for

85 atmospheric CO$_2$ (Nomura et al., 2010; Geilfus et al., 2012; Nomura et al., 2013; Geilfus et al., 2015).

86 Melting sea ice stratifies surface seawater leading to decreased TA, TCO$_2$ and pCO$_2$, in the sea surface,

87 enhancing air-sea CO$_2$ fluxes (Rysgaard et al., 2007; 2009).

Although we now have a basic understanding of the key mechanisms of carbon cycling in sea ice, significant unknowns remain. One of the major unknowns is the fate of ikaite, $T\mathrm{CO_2}$ and $\mathrm{CO_2}$ released from sea ice during winter. It is unclear what proportion of precipitated ikaite crystals in sea ice remain in the matrix to be released upon melt or what proportion are expelled with brine drainage during ice formation and growth. Examining the chemical signatures of the water column beneath sea ice may provide an indication of the importance of the different processes. However, the signal of carbon components released from 1-2 meters of sea ice growth is difficult to detect in a water column several hundred meters deep.

In this study, we followed the evolution of the inorganic carbon dynamics within experimental sea ice from sea ice formation to melt in a sea ice-seawater mesocosm pool (~435 m^3). The benefits of this type of environment are multiple. An artificial pool equipped with a movable bridge makes it possible to collect undisturbed samples from thin growing sea ice. We gain the ability to carefully track carbonate parameters in the ice, in the atmosphere, and in the underlying seawater, while growing sea ice in a large volume of seawater, so that conditions closely mimic the natural system. During this experiment, we examined physical and chemical processes, in the absence of biology, responsible for changes in the inorganic carbon system of sea ice and the underlying seawater and quantify fluxes of inorganic carbon between the atmosphere, sea ice and the water column. We also discuss that dissolution of ikaite crystals exported from sea ice in the underlying seawater can potentially hamper the effect of oceanic acidification on $\Omega_{\mathrm{aragonite}}$.

3. **Site description, sampling and analysis**

The Sea-ice Environmental Research Facility (SERF) is an in-ground outdoor concrete pool of 18.3 m by 9.1 m in surface area and 2.6 m deep exposed to ambient temperatures, winds and solar radiation (by retracting its roof, Fig. 1). The weather conditions in the region are conducive to sea ice growth for several months every winter. Prior to the experiment, the pool is filled with artificial seawater (ASW) made by dissolving large quantities of various rock salts into local groundwater to mimic the major composition of natural seawater (see Rysgaard et al., (2014) for exact composition of the ASW). Sea ice is melted in the pool by circulating heated ethylene glycol through a closed-loop hose located at the bottom of the pool, allowing successive ice growth/melt experiments to be carried out during one winter. The experimental sea ice and brine exhibit similar physical and chemical properties to those observed in natural Arctic sea ice (Geilfus et al., 2013; Hare et al., 2013). The experiment described herein was

120 initiated from open water conditions on 11 January 2013 when the heater was turned off. Sea ice grew

121 until 26 January when the heat was turned back on. The experiment ended on 30 January when the pool

122 was 20% ice-free.

123 Four 375 W pumps were installed on the bottom of the pool near each of the corners to induce a

124 consistent current. The pumps were configured to draw water from their base and then propel it outward

125 parallel to the bottom of the pool. The pumps were oriented successively at right angles to one another,

126 which created a counterclockwise circulation of 2-3 cm s^{-1} (Else et al., 2015).

127 Bulk ice and seawater temperatures were recorded by an automated type-T thermocouple array fixed

128 vertically in the pool. Seawater salinity was measured continuously using Aanderaa CT sensors (model

129 4319) located at 30, 100, 175 and 245 cm depth. The in situ seawater pCO$_2$ was measured every 5 sec

130 using a Contros HydroC (resolution < 1 µatm, accuracy ± 1% of the upper range value) located at 1.3 m

131 depth.

132 Air temperature and relative humidity were measured using a Vaisala HMP45C probe at a

133 meteorological station located 2 m above the sea ice surface. Solar irradiance was continuously recorded

134 by an Eppley Precision Spectral Pyranometer (range=0.285–2.8 µm) mounted 10 m above the sea ice

135 surface. In addition, estimated photosynthetically active radiation (PAR) values at the ice bottom were

136 recorded with Alec mkv-L PAR sensors throughout the study and ranged from 0 to 892 µmol photons m^{-2}

137 s^{-1}.

138 Sea ice and seawater samples were obtained from a confined area located on the North side of the

139 pool to minimize effects on other experiments (e.g. Else et al., 2015). Ice samples were collected using

140 ceramic knives or a Kovacs Mark II coring system depending on the ice thickness. Sampling was

141 performed from a movable bridge to avoid walking on the ice surface and to ensure only undisturbed sites

142 were sampled. Ice cores were collected from one end of the pool (half meter away from the edge of the

143 pool) and at least 20 cm away from previous cored sites. Ice cores were packed in clean plastic bags and

144 kept frozen during the 20 minutes transport to a cold laboratory and processed within a few hours.

145 Seawater was sampled for total alkalinity (TA) and total dissolved inorganic carbon (TCO$_2$) with a

146 peristaltic pump (Cole Palmer, Masterflex-Environment sampler, equipped with PTFE tubing) through an

147 ice core hole the ice-water interface, at 1.25 m, and 2.5 m depth. Samples were stored in 12 ml gas-tight

148   vials (Exetainer, Labco High Wycombe, UK) and poisoned with 12 μl of saturated $HgCl_2$ solution and

149   stored in the dark at 4°C until analysed.

150   Air-ice CO_2 fluxes were measured using a Li-Cor 8100-103 chamber associated with a LI-8100A soil

151   CO_2 flux systems. The chamber was connected in a closed loop to the IRGA with an air pump rate of 3 L

152   min^{-1}. The measurement of pCO_2 in the chamber was recorded every sec over a 15 minute period. The

153   flux was computed from the slope of the linear regression of pCO_2 against time (r^2>0.99) according to

154   Frankignoulle (1988), taking into account the volume of ice or snow enclosed within the chamber. The

155   uncertainty of the flux computation due to the standard error on the regression slope was on average ±3%.

156   In the cold laboratory, sea ice cores were cut into 2 cm sections using a pre-cleaned stainless steel

157   band saw. Each section was placed in a gas-tight laminated (Nylon, ethylene vinyl alcohol and

158   polyethylene) plastic bag (Hansen et al., 2000) fitted with a gastight Tygon tube and a valve for sampling.

159   The plastic bag was sealed immediately and excess air was gently removed through the valve using a

160   vacuum pump. The bagged sea ice samples were then melted in the dark at 4°C to minimize the

161   dissolution of calcium carbonate precipitates (meltwater temperature never rose significantly above 0°C).

162   Once melted, the meltwater mixture and bubbles were transferred to gas-tight vials (12 ml Exetainer,

163   Labco High Wycombe, UK), poisoned with 12 μl solution of saturated $HgCl_2$ and stored in the dark at

164   4°C until analysed.

165   Bulk ice and seawater salinities were measured using a Thermo Orion 3-star with an Orion

166   013610MD conductivity cell and values were converted to bulk salinity (Grasshoff et al., 1983). TA was

167   determined by potentiometric titration (Haraldsson et al., 1997) while TCO_2 was measured on a

168   coulometer (Johnson et al., 1987). Routine analysis of Certified Reference Materials provided by A. G.

169   Dickson, Scripps Institution of Oceanography, verified that TA and TCO_2 were analyzed within ±3 and

170   ±2 μmol kg^{-1}, respectively. Brine volume was estimated from measurements of bulk salinity, temperature

171   and density according to Cox and Weeks (1983) for temperatures below -2°C and according to

172   Leppäranta and Manninen (1988) for ice temperatures within the range -2 to 0°C.

173   Bulk ice samples for biological measurements were collected between 14 and 21 January. Filtered

174   (0.2 μm) SERF seawater (FSW) was added at a ratio of 3 parts FSW to 1 part ice and the samples were

175   left to melt in the dark. Chlorophyll *a* was determined on three occasions by filtering two aliquots of the

176   melted ice sample onto GF/F filters (Whatmann brand) and extracting pigments in 10 ml of 90% acetone

177   for 24 h. Fluorescence was measured before and after the addition of 5% HCl (Turner Designs

178   Fluorometer) and Chl *a* concentration was calculated following Parsons et al. (1984). Measurements of

179   bacterial production were done four times during the biological sampling period by incubating 6-10 ml

180   subsamples of the ice-FSW solution with ^{3}H-leucine (final concentration of 10 nM) for 3h at 0°C in

181   darkness (Kirchmann, 2001). Half of the samples were spiked with trichloroacetic acid (TCA, final

182   concentration 5%) as controls prior to the incubation, while the remaining active subsamples were fixed

183   with TCA (final concentration 5%) after incubation. Following the incubation, vials were placed in 80°C

184   water for 15 minutes (Garneau et al., 2006) before filtration through 0.2 μm cellulose acetate membranes

185   (Whatmann brand) and rinsing with 5% TCA and 95% ethanol. Filters were dried and dissolved in

186   scintillation vials by adding 1 ml ethyl acetate, and radioactivity was measured on a liquid scintillation

187   counter after an extraction period of 24 h. Bacterial production was calculated using the equations of

188   Kirchman (1993) and a conversion factor of 1.5 kg C mol^{-1} (Ducklow et al., 2003).

189   **4. Results**

190   **4.1. Sea ice and seawater physical conditions**

191   Sea ice was grown in the pool from open water on 13 January 2013 and reached a maximum thickness

192   of 24 cm on 26 January at which point the heat at the base of the pool was turned on. On 30 January the

193   experiment ended with the pool 20% ice-free. Three main snowfall events occurred during the

194   experiment. The first, from 14 to 15 January, covered the sea ice surface with 1 cm of snow. The second,

195   from 18 to 23 January, deposited 6-9 cm of snow over the entire pool. On the morning of 23 January, the

196   snow was manually cleared off the ice surface to investigate the insulating effect of the snow on the ice

197   temperature and ikaite precipitation (Rysgaard et al., 2014). Finally, from noon on 24 January to 27

198   January, 8 cm of snow covered the entire pool until the end of the experiment on 30 January.

199   The air temperature at the beginning of the experiment ranged from -2°C to -26°C, which initiated

200   rapid sea ice growth to 15 cm until 18 January (Fig. 2). During this initial sea ice growth, the sea ice was

201   attached to the side of the pool resulting in the development of a hydrostatic pressure head that caused

202   percolation of seawater at the freezing point upwards through the sea ice volume as the sea ice grew

203   downwards. This resulted in repeated events of increased sea ice temperature from the bottom to the

204   surface observed between 15 and 18 January (Fig. 2). Subsequently, the ice was cut using an ice saw

205   around the perimeter, allowing the ice to float and a pressure release valve was installed to prevent such

206   events (Rysgaard et al., 2014). During this period, the ice temperature oscillated between relatively warm

207   (~ -3°C) and cold (~ -7°C) phases. Brine volume content (0.047) was low in the middle part of the ice

208   cover, close to the permeability threshold of 0.05 as suggested by Golden et al., (2007). The bulk ice

209   salinity profiles were typically C-shaped with values ranging from 6 to 23 (Fig. 2). The underlying

210   seawater salinity increased rapidly due to sea ice growth. From 18 to 23 January, the 9 cm snow cover

211   insulated the ice cover from the cold atmosphere (Rysgaard et al., 2014), resulting in a fairly constant ice

212   thickness, nearly no change in ice temperature and salinity, a brine volume content above the

213   permeability threshold and a small increase in the underlying seawater salinity. Once the ice surface was

214   cleared of snow on the morning of 23 January, the ice temperature decreased throughout the entire ice

215   thickness and the ice surface salinity increased. The sea ice volume cooled from the top downwards, and

216   the brine volume content decreased below the permeability threshold on 23 January and rapid sea ice

217   growth rapidly increased the seawater salinity. Shortly after the snow clearing, the last snowfall event

218   covered the ice surface with 8 cm of snow, reducing the effect of the cold atmosphere on the ice cover.

219   On 26 January, the heater was activated to initiate sea ice melt. Sea ice temperatures increased and

220   became isothermal around -2°C while the bulk ice salinity decreased and the brine volume content

221   increased up to 0.13. The sea ice melt decreased the seawater salinity. The pool was well mixed during

222   the whole growth phase with similar salinity and temperature observed at the four depths. However, once

223   the heat was turned on, the pool become stratified with respect to salinity changes, as the salinity at 30 cm

224   depth started to diverge from the deeper depths (Fig. 2).

225   **4.2. Carbonate system**

226   TA and $T\mathrm{CO}_2$ in seawater, noted as $\mathrm{TA}_{(sw)}$ and $T\mathrm{CO}_{2(sw)}$, were sampled at the sea ice-seawater

227   interface, 1.25 and 2.5 m depth. An ANOVA test over the 3 depths revealed that the means are not

228   statistically different (p<0.01) so we consider the average concentration of the three depths in the

229   following analysis. During sea ice growth, $\mathrm{TA}_{(sw)}$ increased from 2449 to 2644 µmol kg^{-1} (black line, Fig.

230   3a) while $T\mathrm{CO}_{2(sw)}$ increased from 2347 to 2516 µmol kg^{-1} (black line, Fig. 3b). Once the ice started to

231   melt, $\mathrm{TA}_{(sw)}$ decreased to 2607 µmol kg^{-1} and $T\mathrm{CO}_{2(sw)}$ decreased to 2461 µmol kg^{-1}. As the experiment

232   stopped before the ice was completely melted in the tank, both the seawater salinity and $\mathrm{TA}_{(sw)}$ do not

233   reach their initial values at the end of the experiment (Table 1, Fig 2 and 3). To discard the effect of

234   salinity changes, we normalized $\mathrm{TA}_{(sw)}$ and $T\mathrm{CO}_{2(sw)}$ to a salinity of 33 (noted as $n\mathrm{TA}_{(sw)}$ and $nT\mathrm{CO}_{2(sw)}$)

235   according to the equations 4 and 5:

236 $$nTA_{(sample)\,t} = \frac{TA_{(sample)\,t}}{S_{(sample)\,t}} \times 33 \qquad\qquad (4)$$

237 $$nTCO_{2\,(sample)\,t} = \frac{TCO_{2\,(sample)\,t}}{S_{(sample)\,t}} \times 33 \qquad\qquad (5)$$

238 where t is the time of the sampling and S the salinity of the sample (seawater or sea ice). During ice

239 growth, $nTA_{(sw)}$ and $nTCO_{2(sw)}$ increased slightly to 2446 and 2328 µmol kg^{-1}, respectively (Fig. 3c).

240 However, once the ice started to melt, $nTA_{(sw)}$ increased to 2546 µmol kg^{-1} and $nTCO_{2(sw)}$ increased to

241 2404 µmol kg^{-1}.

242 The in situ pCO_2 of the underlying seawater ($pCO_{2(sw)}$) decreased from 377 to 360 µatm as the

243 seawater temperature in the pool decreased to the freezing point. The $pCO_{2(sw)}$ then oscillated from 360 to

244 365 µatm during sea ice growth. One day after the heater was turned on, the $pCO_{2(sw)}$ increased to a

245 similar concentration as at the beginning of the experiment before decreasing to 373 µatm by the end of

246 the experiment (Fig. 3d).

247 Within bulk sea ice, $TA_{(ice)}$ ranged from 300 to 1907 µmol kg^{-1} while $TCO_{2(ice)}$ ranged from 237 to

248 1685 µmol kg^{-1}. Both $TA_{(ice)}$ and $TCO_{2(ice)}$ exhibited C-shaped profiles with higher concentrations at the

249 surface and bottom layers of the ice cover (Fig. 4). The concentration of $TA_{(ice)}$ (average = 476 µmol kg^{-1})

250 and $TCO_{2(ice)}$ (average = 408 µmol kg^{-1}) did not show significant variability during our survey, except at

251 the surface of the ice. A first maximum was observed on 17 January with concentration of 1907 µmol kg^{-1}

252 for TA and 1685 µmol kg^{-1} for TCO_2. A second maximum was observed on 23 January with

253 concentration of 1433 µmol kg^{-1} for TA and 861 µmol kg^{-1} for TCO_2. These maxima matched the high

254 bulk ice salinity (Fig. 2), so we also normalized $TA_{(ice)}$ and $TCO_{2(ice)}$ (noted as $nTA_{(ice)}$ and $nTCO_{2(ice)}$, Fig.

255 4) to a salinity of 33 (according to the equations 4 and 5) to discard the effect of salinity changes and

256 facilitate comparison with the underlying seawater. During initial sea ice formation (up to 17 January),

257 the concentration of both $nTA_{(ice)}$ (from 1083 to 2741, average = 1939 µmol kg^{-1}) and $nTCO_{2(ice)}$ (from

258 853 to 2440, average = 1596 µmol kg^{-1}) were at their minima in the experimental time series. From 17 to

259 21 January, both $nTA_{(ice)}$ and $nTCO_{2(ice)}$ increased throughout the ice column (average $nTA_{(ice)}$ = 2375

260 µmol kg^{-1} and $nTCO_{2(ice)}$ = 2117 µmol kg^{-1}). However, from 21 January until the initial sea ice melt,

261 $nTA_{(ice)}$ and $nTCO_{2(ice)}$ decreased in the top 5 cm of the ice cover (average $nTA_{(ice)}$ = 2125 µmol kg^{-1} and

262 $nTCO_{2(ice)}$ = 1635 µmol kg^{-1}).

263 **4.3. Air-ice CO$_2$ fluxes**

264   The CO$_2$ fluxes measured at the variably snow-covered sea ice surface (Fig. 2b), ranged from 0.29 to

265   4.43 mmol m^{-2} d^{-1} show that growing sea ice released CO$_2$ to the atmosphere (Fig. 5). However, as soon

266   as the ice started to warm up and then melt, the sea ice switched from source to sink for atmospheric CO$_2$

267   with downward fluxes from -1.3 to -2.8 mmol m^{-2} d^{-1}. These ranges of air-ice CO$_2$ exchanges are of the

268   same order of magnitude as fluxes reported on natural sea ice using the same chamber technique in the

269   Arctic during the initial sea ice growth (from 4.2 to 9.9 mmol m^{-2} d^{-1} in Geilfus et al., 2013) and during

270   the spring-summer transition (from -1.4 to -5.4 mmol m^{-2} d^{-1} in Geilfus et al., 2015). In Antarctica air-ice

271   CO$_2$ fluxes were reported during the spring-summer transition from 1.9 to -5.2 mmol m^{-2} d^{-1} by Delille et

272   al (2014), from 0.3 to -2.9 mmol m^{-2} d^{-1} (Geilfus et al., 2014) and from 0.5 to -4 mmol m^{-2} d^{-1} (Nomura et

273   al., 2013).

274   **5. Discussion**

275   **5.1. Key processes affecting the carbonate system**

276   The dynamics of inorganic carbon in the ocean and sea ice are mainly affected by temperature and

277   salinity changes, precipitation and dissolution of calcium carbonate, and biological activities (Zeebe and

278   Wolf-Gladrow, 2001). During this experiment, neither organic matter nor biota were purposely

279   introduced into the pool; the observed range of bulk ice microbial activity (5.7 x 10^{-9} on 14 January to 7.5

280   x 10^{-7} g C L^{-1} h^{-1} on 21 January) and algal Chl a (0.008 on 14 January to 0.002 µg L^{-1} on 21 January) were

281   too low to support any biological activity (Rysgaard et al., 2014). Therefore biological activity is unlikely

282   to have played a role. During the same 2013 time series at SERF, Rysgaard et al. (2014) discussed the

283   precipitation of ikaite within the ice cover in detail, reporting high concentrations of ikaite (> 2000 µmol

284   kg^{-1}) at the surface of the ice in brine skim and frost flowers and ikaite precipitation up to 350 µmol kg^{-1}

285   within bulk sea ice. Within sea ice, ikaite precipitation is associated with low ice temperatures, high bulk

286   salinity and high TA$_{(ice)}$ and TCO$_{2(ice)}$ concentrations (Fig. 2 and 3).

287   The main processes affecting the carbonate system can be described by changes in TA and TCO$_2$

288   (Zeebe and Wolf-Gladrow, 2001). An exchange of CO$_{2(gas)}$ affects TCO$_2$ while TA remains constant and

289   the precipitation-dissolution of calcium carbonate affects both TA and TCO$_2$ in a ratio of 2:1 (see

290   equation 1 to 3, Fig. 6). To calculate the theoretical changes in TA and TCO$_2$ during the course of the

291   experiment, we used seawater samples from 11 January prior to sea ice formation (t=0, Table 1) as the

292   origin point (blue circle on Fig. 6). Sea ice data are located between the theoretical calcium carbonate

293   precipitation line and the CO$_2$ release line (Fig. 6a) while seawater data mainly fall on the calcium

294   carbonate dissolution line (Fig. 6b), suggesting that the carbonate system within sea ice is affected by

295   both the precipitation of ikaite and a release of $CO_{2(gas)}$ while the underlying seawater is mainly affected

296   by the dissolution of calcium carbonate.

297   **5.2. Estimation of the precipitation-dissolution of ikaite**

298   During the experiment, Rysgaard et al., (2014) observed ikaite within sea ice using direct microscopic

299   observations. The precipitation-dissolution of ikaite and gas exchange are the only two processes taking

300   place during the experiment. As illustrated in Fig. 6, an exchange of CO_2 does not affect TA while the

301   precipitation-dissolution of ikaite affects TA and TCO_2 in a ratio 2:1. Therefore, we use TA to estimate

302   how much ikaite is precipitated or dissolved within the ice cover and the underlying seawater.

303   Assuming no biological effect, ikaite precipitation/dissolution and gas exchange, TA and TCO_2 are

304   considered conservative with salinity. Therefore, we can calculate the expected TA and TCO_2 (noted as

305     $TA_{(ice)}^{*}$ and $TCO_{2(ice)}^{*}$ in the ice cover and $TA_{(sw)}^{*}$, $TCO_{2(sw)}^{*}$ for the water column) based on the initial

306   seawater conditions ($TA_{(sw)}$, $TCO_{2(sw)}$ and $S_{(sw)}$ at t=0, Table 1) and the sample salinity (bulk sea ice or

307   seawater) measured during the experiment:

308
$$TA_{(sample)\,t}^{*} = \frac{TA_{(sw)\,t=0}}{S_{(sw)\,t=0}} \times S_{(sample)\,t} \qquad\qquad (6)$$

309
$$TCO_{2\,(sample)\,t}^{*} = \frac{TCO_{2\,(sw)\,t=0}}{S_{(sw)\,t=0}} \times S_{(sample)\,t} \qquad\qquad (7)$$

310   where t is the time of the sampling. Within the ice cover, $TA_{(ice)}$, $TCO_{2(ice)}$, and the bulk ice salinity are

311   averaged throughout the ice column at each sampling day (Fig. 7a, b, black line) while for the underlying

312   seawater, we used the averaged $TA_{(sw)}$, $TCO_{2(sw)}$ and salinity for all the measured depths (Fig. 2a, b, black

313   line). The difference between $TA_{(sample)}^{*}$ and the observed TA is only due to the precipitation or

314   dissolution of ikaite crystals. In case of ikaite precipitation (*i.e.* $TA_{(sample)}^{*} > TA_{(sample)}$), half of this

315   positive difference corresponds to the amount of ikaite precipitated within the ice. This ikaite may either

316   remain or may be exported out of the ice. A negative difference (*i.e.* $TA_{(sample)}^{*} < TA_{(sample)}$), indicates

317   ikaite dissolution.

318   **5.2.1. Sea ice**

319   Greater $TA_{(ice)}^{*}$ and $TCO_{2(ice)}^{*}$ compared to the averaged observed $TA_{(ice)}$ and $TCO_{2(ice)}$ (Fig. 7a, b) are

320   expected as ikaite is precipitated and CO_2 released from the ice to the atmosphere (Fig. 5, 6). Half the

321   difference between $TA_{(ice)}^{*}$ and $TA_{(ice)}$ is a result of ikaite precipitation (Fig. 7c, black diamonds). Highly

Nicolas-Xavier Geilfus 12/7/2016 12:43
Deleted: dots

323 variable ikaite precipitation was observed (Fig. 7c). Ikaite precipitation was up to 167 µmol kg^{-1} (e.g. first

324 days of the experiment) and as low as 1 µmol kg^{-1} (e.g. 19 January). A negative difference between

325 TA$_{(ice)}$* and TA$_{(ice)}$ (*i.e.* ikaite dissolution) occurred on three occasions: 14, 20 and after the 26 January

326 (beginning of the sea ice melt). On these occasions, the ice cover was relatively warm due to warmer

327 atmospheric temperatures (14 January), thicker snow cover insulating the ice cover from the cold

328 atmosphere (20 January) or when heat was turned back on (after 26 January, Fig. 2). Relatively high sea

329 ice temperatures likely promote ikaite dissolution in agreement with Rysgaard et al., (2014) who linked

330 ikaite precipitation/dissolution to ice temperature. The upward percolation of seawater observed from 15

331 to 18 January might complicate the effect of sea ice temperature on ikaite formation because it was in part

332 responsible for increased ice temperatures (Fig. 2b) and therefore increased the sea ice brine volumes

333 (Fig. 2c). Increased vertical connectivity (permeability) of the network of liquid inclusions throughout the

334 sea ice (Golden et al., 2007; Galley et al., 2015) would have allowed the export of ikaite crystals from the

335 ice cover to the underlying seawater. However, while we calculated a negative difference between TA$_{(ice)}$*

336 and TA$_{(ice)}$, ikaite crystals were observed by Rysgaard et al., (2014). We compared the direct microscopy

337 observations by averaging the amount of ikaite precipitated throughout the ice thickness for each

338 sampling day from Rysgaard et al., (2014) (Fig. 7c, white dots) with our estimation of the amount of

339 ikaite based on the difference between TA$_{(ice)}$* and TA$_{(ice)}$ (Fig. 7c, black diamonds). Both ikaite

340 measurements are of the same order of magnitude however the average (22 µmol kg^{-1}) and maximum

341 (100 µmol kg^{-1}) of direct observations presented by Rysgaard et al. (2014) were lower than our estimated

342 average (40 µmol kg^{-1}) and maximum of up to 167 µmol kg^{-1} over this whole experiment. Deviations are

343 likely due to methodological differences. Here, sea ice samples were melted to subsample for TA and

344 TCO$_2$, Ikaite crystals may have dissolved during melting, leading to an underestimation of the total

345 amount of ikaite precipitated in the ice. However, the difference between TA$_{(ice)}$* and TA$_{(ice)}$ provides an

346 estimation of how much ikaite is precipitated in the ice cover, including those crystals potentially already

347 exported to the underlying seawater. The method used by Rysgaard et al., (2014) avoid the bias of ikaite

348 dissolution during sea ice melt with the caveat that crystals need to be large enough to be optically

349 detected. If no crystals were observed, Rysgaard et al., (2014) assumed that no crystals were precipitated

350 in the ice, though ikaite crystals could have been formed and then exported into the underlying seawater

351 prior to microscopic observation of the sample, which may explain the difference observed between both

352 methods during initial sea ice formation (15-18 January) when the ice was still very thin. In addition, the

Nicolas-Xavier Geilfus 12/7/2016 12:51
Deleted: dots

succession of upward percolation events could have facilitated the ikaite export from the ice cover to the underlying seawater. Estimations from both methods show similar concentrations when the ice (i) warmed due to snowfall (18-23 January) and (ii) cooled once the snow was removed (on 23 January). Once the ice started to melt (26 January), Rysgaard et al., (2014) reported a decrease in the ikaite precipitation while in this study we reported a negative difference between $TA_{(ice)}^*$ and $TA_{(ice)}$, possibly indicating that ikaite dissolved in the ice.

5.2.2. Water column

The main process affecting the carbonate system in the underlying seawater in this study is the export of ikaite from the ice and its dissolution in the water column (Fig. 6). While a few studies of ikaite precipitation within sea ice carried out over open ocean hypothesized that ikaite remained trapped within the sea ice matrix (Rysgaard et al., 2007; 2013; Delille et al., 2014), the observed increase of $nTA_{(sw)}$ (Fig. 3) suggests that ikaite precipitated within the ice cover was exported to the underlying seawater where the crystals were dissolved as suggested by Fransson et al., (2013). Lower $TA_{(sw)}^*$ and $TCO_{2(sw)}^*$ compared to $TA_{(sw)}$ and $TCO_{2(sw)}$ (Fig. 3) confirm the dissolution of ikaite in the underlying seawater as the dissolution of ikaite crystals will decrease both TA and TCO_2 (equations 1 to 3). Therefore, half the difference between $TA_{(sw)}^*$ and $TA_{(sw)}$ corresponds to the concentration of ikaite exported from the ice and dissolved in the underlying seawater (Fig. 8a). This concentration increased over time to a maximum of 66 µmol kg^{-1}.

During this experiment, $nTA_{(sw)}$ increased by 128 µmol kg^{-1} while $nTCO_{2(sw)}$ increased by 82 µmol kg^{-1} (Fig. 3c). This suggests that 64 µmol kg^{-1} of ikaite are dissolved compared to the 66 µmol kg^{-1} estimated from the difference between $TA_{(sw)}^*$ and $TA_{(sw)}$. As a result of the effect of ikaite dissolution on the 2:1 ratio of $TA:TCO_2$, the dissolution of ikaite accounts for the entire increase of $nTA_{(sw)}$ but only accounts for 64-66 µmol kg^{-1} of the 82 µmol kg^{-1} increase in $nTCO_{2(sw)}$. So, 16-18 µmol kg^{-1} (about 25%) of the increase of $nTCO_{2(sw)}$ cannot be explained by the dissolution of ikaite. The increase of both $nTA_{(sw)}$ and $nTCO_{2(sw)}$ is more significant once the ice starts to melt (26 January). During sea ice melt, increased vertical permeability resulting in increased liquid communication through the sea ice volume from below likely in part dissolved ikaite crystals still residing in the ice at that time, and also will have created a downward crystal export mechanism. As the ice melt advanced, patches of open water occurred at the surface of the pool. Therefore, uptake of atmospheric CO_2 by the undersaturated seawater likely occurred, increasing the $TCO_{2(sw)}$.

385   The dissolution of ikaite crystals could also have a strong impact on the $p\text{CO}_{2(sw)}$. The water column

386   was undersaturated compared to the atmosphere during the whole experiment (Fig. 3d). A release of CO_2,

387   from the ice to the atmosphere was measured during sea ice growth (Fig. 5) in spite of the undersaturated

388        $p\text{CO}_{2(sw)}$. This suggests that air-ice CO_2 fluxes are only due to the concentration gradient between the ice

389   and the atmosphere (Geilfus et al., 2012; Nomura et al., 2013) but that sea ice exchanges CO_2 with the

390   atmosphere independently of the seawater concentration (Geilfus et al., 2014). The $p\text{CO}_{2(sw)}$ is highly

391   correlated with the seawater temperature (Fig. 2) with a rapid decrease of $p\text{CO}_{2(sw)}$ during the first days of

392   the experiment (13 to 15 January) and a relative constant $p\text{CO}_{2(sw)}$ until 27 January. However, on 26

393   January, the heat was turned back on affecting the seawater temperature on the same day (Fig. 2) while

394   the impact of increasing temperature on the $p\text{CO}_{2(sw)}$ appeared one day later (Fig. 3d). We normalized the

395        $p\text{CO}_{2(sw)}$ to a temperature of -1°C (after Copin-Montegut (1988), noted as $np\text{CO}_{2(sw)}$, blue line on Fig. 3d).

396   The $np\text{CO}_{2(sw)}$, does not show major variations during sea ice growth with values around 380 µatm.

397   However, once the heat is turned on and the seawater temperature increased (on 26 January), $np\text{CO}_{2(sw)}$

398   decreased from 383 µatm to 365 µatm, while $p\text{CO}_{2(sw)}$ did not change in response to increased seawater

399   temperatures until 27 January, suggesting that a process other than temperature change affected the

400        $p\text{CO}_{2(sw)}$. According to equation 1, the dissolution of calcium carbonate has the potential to reduce

401        $p\text{CO}_{2(sw)}$. Therefore, during sea ice growth and the associated release of salt, TA, $T\text{CO}_2$ and ikaite crystals

402   to the underlying seawater, ikaite dissolution within the seawater could be responsible for maintaining

403   stable $p\text{CO}_{2(sw)}$ values while seawater salinity, $\text{TA}_{(sw)}$ and $T\text{CO}_{2(sw)}$ are increasing. Once the seawater

404   temperature increased (26 January), sea ice melt likely released ikaite crystals to the underlying seawater

405   (Fig. 2, 8a) along with brine and meltwater, a process that would continuously export ikaite from the sea

406   ice as the volume interacting with the seawater via percolation or convection increased. The dissolution of

407   these crystals likely contributed to keeping the $p\text{CO}_{2(sw)}$ low and counterbalancing the effect of increased

408   temperature. We argued that once all the ikaite crystals are dissolved, the increase seawater temperature

409   increased the $p\text{CO}_{2(sw)}$ simultaneously with the $np\text{CO}_{2(sw)}$ (27 January, Fig. 3).

410   **5.3. Ikaite export from the ice cover to the water column**

411   We estimated the amount of ikaite precipitated and dissolved within sea ice and seawater based on the

412   sea ice (and seawater) volume (in m^3), the sea ice and seawater density, the concentration of ikaite

413   precipitated and dissolved within the ice cover (Fig. 7c), and the concentration of ikaite dissolved in the

414   water column (Fig. 8a). Within the ice cover, the amount of ikaite precipitated-dissolved ranged from -0.7

to 1.97 mol (Fig 8b, Table 2), with a maximum just after the snow was cleared on 23 January. In the underlying seawater, the amount of ikaite dissolved in the pool increased from 0.47 mol on the first day of the experiment to 11.5 mol on 25 January when sea ice growth ceased. Once the ice started to melt the amount of dissolved ikaite increased up to 20.9 (28 Jan) and 26.7 mol (29 January, Table 2). The estimation of ikaite dissolution in the pool is significantly higher than the estimated amount of ikaite precipitated (and potentially exported) within the ice cover, especially during sea ice melt. Within the ice cover, the ikaite values presented here represent a snapshot of the ikaite content in the ice at the time of sampling. In the underlying seawater, ikaite dissolution increased $TA_{(sw)}$ cumulatively over time.

The difference between $TA_{(ice)}^*$ and $TA_{(ice)}$ provides an estimation of ikaite precipitated within the ice, including potential ikaite export to the underlying seawater, so it cannot be used to determine how much ikaite remained in the ice versus how much dissolved in the water column. However, Rysgaard et al., (2014) indicate ikaite precipitated within the ice based on direct observations. Using the ikaite concentration reported in Rysgaard et al (2014) (and shown in Fig. 7c), the sea ice volume (in m^3) and density, we calculate that 0 to 3.05 mol of ikaite precipitated within the ice cover during sea ice growth (Fig. 8b and Table 2). This amount decreased to 0.46 and 0.55 mol during the sea ice melt (28 and 29 January, respectively). Increased ikaite dissolution in the water column when the ice began to melt (from 11.5 to 20.9 mol) indicates that 9.4 mol of ikaite were stored in the ice and rejected upon the sea ice melt. This amount is about three times the amount of ikaite precipitated in the ice estimated by Rysgaard et al., (2014) at the end of the growth phase (3.05 mol, Table 2), suggesting more work is needed best estimate ikaite precipitation within sea ice.

Once the ice started to melt, the increased ikaite dissolution from 11.5 mol to 20.9 mol (28 January) and to 26.7 mol (29 January) suggests that about the same amount of ikaite is dissolved during the sea ice growth as during the first two days of the sea ice melt. The amount of ikaite dissolved in the water column after melt commenced continued to increase cumulatively, suggesting that ikaite is continuously exported to the underlying seawater as increased sea ice temperatures permit more of the volume to communicate with the underlying seawater. Therefore, we can assume than more than half of the amount of ikaite precipitated within the ice remained in the ice cover before ice melt began.

5.4. Air-ice-seawater exchange of inorganic carbon

443   SERF is a semi-closed system where the only way for the surface (water or sea ice) to gain or lose CO_2

444   is through exchange with the atmosphere, making it reasonable to track the exchange of TCO_2 in the

445   atmosphere-sea ice-seawater system. The ice cover always had lower $TCO_{2(ice)}$ during the experiment

446   ($TCO_{2(ice)}^{*} > TCO_{2(ice)}$) compared to what would be expected if the CO_2 simply followed brine rejection in

447   a conservative process (i.e. $TCO_{2(ice)}^{*}$) (Fig. 7b). This could be due to: (i) CO_2 released to the atmosphere

448   from sea ice, (ii) decreased $TCO_{2(ice)}$ due to the precipitation of ikaite within sea ice and/or (iii) sea ice

449   exchanging TCO_2 with the underlying seawater.

450   The number of moles of TCO_2 exchanged during this experiment was calculated using the sea ice (and

451   seawater) volume (in m^3) and density (in kg/m^3). The total amount of $TCO_{2(ice)}$ lost from the ice cover (the

452   difference between $TCO_{2(ice)}^{*}$ and $TCO_{2(ice)}$) ranged from 0.11 to 6.02 mol (average 2.38 mol, Fig. 9, black

453   dots). The greatest sea ice TCO_2 losses occurred on 15-16 January during initial sea ice growth and from

454   23 to 25 January, during ice cooling due to snow removal. The exchange of CO_2 between the ice and the

455   atmosphere is known (Fig. 5). The number of mole of CO_2 exchanges between the ice and the atmosphere

456   were calculated (noted as $CO_{2(air-ice)}$ in Table 2) using the time step between each flux measurement, the

457   ice thickness and density. During sea ice growth 0.01 to 0.42 mol of CO_2 were released from the ice-

458   covered pool to the atmosphere. During sea ice melt uptake of atmospheric CO_2 by the ice-covered pool

459   ranged from -0.15 to -0.93 (Fig. 9, white triangles). On average, over the duration of the experiment, the

460   ice cover released 0.08 mol of CO_2 to the atmosphere. Assuming we know how much ikaite is contained

461   within the ice cover (Fig. 8b), we can estimate how much TCO_2 is exported from the ice to the underlying

462   seawater (Fig. 9, blue triangles) by subtracting the air-ice CO_2 exchange and the ikaite precipitation from

463   the total reduction of $TCO_{2(ice)}$ observed within the ice cover (Fig. 9, black dots). The sea ice-to-seawater

464   TCO_2 export ranged from 0.2 to 3.98 mol (average = 1.7 mol), confirming that sea ice primarily exports

465   TCO_2 to the underlying seawater. TCO_2 export from the ice to the water column ranged from 23% of the

466   total sea ice TCO_2 early in the ice growth (14 January) to 100% after the onset of melt. These estimations

467   are comparable to the study of Sejr et al., (2011) who suggested that sea ice exports 99% of its total TCO_2

468   to the seawater below it. On average over the whole experiment, sea ice exported 1.7 mol of TCO_2 to the

469   underlying seawater (Fig. 9), which corresponds to a $TCO_{2(sw)}$ increase of 43.5 $\mu mol\ kg^{-1}$ considering the

470   average sea ice thickness and density during the experiment and the volume of the pool. However,

471     $TCO_{2(sw)}$ increased by 115 $\mu mol\ kg^{-1}$ over the whole experiment (Fig. 3b), leaving an increase of 71.5

472     $\mu mol\ kg^{-1}$ in the $TCO_{2(sw)}$ that cannot be explained by the sea ice-seawater exchange of TCO_2. We

473   postulate that as the ice melt advanced, patches of open water that opened at the surface of the pool which

474   were undersaturated compared to the atmosphere (Fig. 3d) imported the additional TCO$_2$ directly from the

475   atmosphere in the form of CO$_{2(g)}$. Considering the pool volume, the 71.5 µmol kg^{-1} increase of TCO$_{2(sw)}$

476   could be explained by an air-sea water CO$_2$ uptake of 8.5 mmol m^{-2} d^{-1} over 3 days of sea ice melt in a

477   20% ice free pool. High air-sea gas exchanges rates have been observed over partially ice-covered seas

478   (Else et al., 2011; 2013). This mechanism is also corroborated by models that account for additional

479   sources of turbulence generated by the presence of sea ice (Loose et al., 2014).

480   The design of the experiment allowed for constrained measurements of inorganic carbon fluxes

481   between sea ice and the water column not possible in a natural environment where large volume, mixing

482   processes alter the underlying seawater making it more complicated to identify changes. We build a CO$_2$

483   budget based only on the sea ice growth phase because only two days of data for the melt phase are

484   available and the experiment stopped while the pool was 20% ice-free (Rysgaard et al., 2014; Else et al.,

485   2015). The initial seawater (origin point, t=0) contained 1040.9 mol of TCO$_{2(sw)}$ on 11 January while on

486   the last day of sea ice growth (25 January) the seawater contained 1017.3 mol of TCO$_{2(sw)}$ (Table 2) with

487   the difference, (23.6 mol of TCO$_2$) in all likelihood transferred from the water column to the ice cover or

488   the atmosphere. However, the TCO$_2$ content within the ice cover at the end of the growing phase was 15.6

489   mol and the ice cover released 3.1 mol of CO$_2$ to the atmosphere (Table 2). Therefore, 4.9 mol of the 23.6

490   mol of TCO$_2$ exchanged from the water column are unaccounted for, but may be explained by air-ice CO$_2$

491   fluxes. The chamber measurement technique for air-ice CO$_2$ flux may underestimate the exchange of

492   CO$_2$, and the air-seawater CO$_2$ fluxes are unknown until the ice started to grow (13 January). These

493   missing moles of TCO$_2$ may also be explained by our assumption of uniform sea ice thickness in the

494   SERF. Using the seawater conditions at the end of the experiment, 1-cm of seawater in the pool contains

495   4.21 mol of TCO$_2$, making it difficult to close our budget.

496   **5.5. Potential impact of sea ice growth and ikaite export on aragonite saturation state of the**

497   **underlying seawater.**

498   The Arctic Ocean is a region where calcifying organisms are particularly vulnerable to ocean

499   acidification since low temperatures and low salinity lower the carbonate saturation state. As a result

500   several areas of the Arctic Ocean are already undersaturated with respect to aragonite (Chierici and

501   Fransson 2009; Yamamoto-Kawai et al., 2009; Bates et al., 2011). This undersaturation is enhanced in

502   winter as the temperature decreases and pCO$_2$ increases as a result of respiration. Calcifying organisms

might therefore be most susceptible to the effects of acidification in the winter, corresponding to the annual minimum in aragonite saturation state ($\Omega_{aragonite}$). Sea ice retreat is thought to enhance the impact of ocean acidification by freshening and ventilating the surface water (Yamamoto-Kawai et al., 2008; Yamamoto et al., 2012; Popova et al., 2014). However, any understanding of the effect of ikaite precipitation in sea ice on ocean acidification is still in its infancy (e.g. Fransson et al., 2013).

Since the discovery of ikaite precipitation in sea ice (Dieckmann et al., 2008), research on its impact on the carbonate system of the underlying seawater has been ongoing. Depending on the timing and location of this precipitation within sea ice, the impact for the atmosphere and the water column in terms of CO_2 transport can be significantly different (Delille et al., 2014). Dissolution of ikaite within melting sea ice in the spring and export of this related high TA:TCO_2 ratio meltwater from the ice to the water column will decrease the pCO_2, increase pH and $\Omega_{aragonite}$ of the surface layer seawater. Accordingly, during sea ice melt, an increase of $\Omega_{aragonite}$ in the surface water in the Arctic was observed (Chierici et al., 2011, Fransson et al., 2013, Bates et al., 2014). However, it was difficult to ascribe this increase to the legacy of excess TA in sea ice, ikaite dissolution or primary production.

The impact of ikaite precipitation on the surface seawater during sea ice growth is less clear. Fransson et al., (2013) suggested in winter in the Amundsen Gulf that the release of brine decreased $\Omega_{aragonite}$ by 0.8 at the sea ice-seawater interface as a result of ikaite precipitation within sea ice and the related CO_2 enrichment of brine. Conversely, during ice melt, $\Omega_{aragonite}$ increased by 1.4 between March and May, likely due to both calcium carbonate dissolution and primary production. This contrasts with the present experiment. Figure 10 shows the evolution of $\Omega_{aragonite}$ and pH in the water column derived from $TA_{(sw)}$ and $TCO_{2(sw)}$ and the evolution of $\Omega_{aragonite}$ and pH predicted solely from salinity changes (i.e. using $TA_{(sw)}^*$ and $TCO_{2(sw)}^*$, noted as $\Omega_{aragonite}^*$ and pH^*). We used the CO2sys_v2.1.xls spreadsheet (Pierrot et al., 2006) with the dissociation constants from Goyet and Dickson (1989) and all other constants from DOE (1994). This shows the complexity of ikaite and its impact on the carbonate system and Ω in the underlying water.

During ice growth, sea ice brine rejection appears to increase both pH (from 8.00 to 8.06) and $\Omega_{aragonite}$ (from 1.28 to 1.65) of the underlying seawater, offsetting the effect of decreased temperature. A slight increase of $\Omega_{aragonite}$ was predicted due to increased salinity and a proportional increase of TA and TCO_2 as depicted in $\Omega_{aragonite}^*$. However, the effect of ikaite rejection and subsequent changes in TA strongly enhance the increase of $\Omega_{aragonite}$. Therefore, ikaite rejection from sea ice has a much stronger potential to

533 increase $\Omega_{aragonite}$ than brine rejection during fall and winter sea ice growth, suggesting ikaite exported to

534 seawater from sea ice may hamper the effect of oceanic acidification on $\Omega_{aragonite}$ in fall and winter in at

535 the time when $\Omega_{aragonite}$ is at its minimum (Chierici and Fransson 2009, Yamamoto-Kawai et al., 2009,

536 Chierici et al., 2011). Ice formation may therefore delay harmful effects of ocean acidification on

537 calcifying organisms by increasing $\Omega_{aragonite}$ in the critical winter period when $\Omega_{aragonite}$ reaches its minimal

538 values. As a corollary, ice removal acts to alleviate the effect of ikaite rejection and may therefore lowers

539 $\Omega_{aragonite}$. This calls for an accounting of under-ice ikaite rejection in modeling predictions on the

540 consequences of Arctic Ocean acidification in the context of northern hemispheric annual multi-year sea

541 ice loss, as increased summer open water will lead to more first year sea ice formation in fall and winter

542 in the future.

543 **6. Conclusion**

544 We quantified the evolution of inorganic carbon dynamics from initial sea ice formation to its melt in

545 a sea ice-seawater mesocosm pool from 11 to 29 January 2013. Based on our analysis of TA and $T\mathrm{CO}_2$ in

546 sea ice and seawater, the main processes affecting inorganic carbon within sea ice are ikaite precipitation

547 and CO_2 exchange with the atmosphere, while in the underlying seawater dissolution of ikaite was the

548 main process affecting the inorganic carbon system.

549 During this experiment, sea ice exchanged inorganic carbon components (e.g. CO_2, ikaite, $T\mathrm{CO}_2$) with

550 both the atmosphere and the underlying seawater. During sea ice growth, CO_2 was released to the

551 atmosphere while during ice melt an uptake of atmospheric CO_2 was observed. We report ikaite

552 precipitation up to 167 µmol kg^{-1} of sea ice, similar to previous estimates from Rysgaard et al., (2014)

553 based on microscopically observed values. In the underlying seawater, a net increase of $n\mathrm{TA}_{(sw)}$ over the

554 whole experiment was observed (up to 128 µmol kg^{-1}), suggesting that a portion of the ikaite crystals

555 precipitated within sea ice were exported to the underlying seawater and then dissolved as the ice cover

556 evolved in time. Ikaite export from ice to the underlying seawater was associated with brine rejection

557 during sea ice growth, increased sea ice vertical connectivity due to the upward percolation of seawater,

558 and meltwater flushing during sea ice melt. Rysgaard et al., (2007) suggested that ikaite precipitation

559 within sea ice could act as a significant sink for atmospheric CO_2, however to act as a sink for

560 atmospheric CO_2, ikaite crystals must remain in the ice structure while the CO_2 produced by their

561 precipitation is expelled with dense brine rejection and entrained in deep seawater (Delille et al., 2014).

562 TA changes observed in the water column once the sea ice started to melt indicate that more than half of

Nicolas-Xavier Geilfus 12/7/2016 13:31
Deleted: impede

Nicolas-Xavier Geilfus 13/7/2016 14:50
Deleted: from open water

the total amount of ikaite precipitated in the ice during the sea ice growth remained in the ice until the sea ice began to melt. Derivation of air-sea CO_2 fluxes related to the sea ice carbon pump should take into account ikaite export to the underlying ocean during sea ice growth, which might reduce the efficiency of oceanic CO_2 uptake upon sea ice melt. As sea ice melts, ikaite is flushed downward out of the ice along with the meltwater.

Ikaite export from sea ice and its dissolution had a strong impact on the underlying seawater. In this semi-closed system, sea ice growth increased the seawater salinity, $TA_{(sw)}$, and $TCO_{2(sw)}$. In spite of those increases, the pCO_2 of the underlying seawater remained undersaturated compared to the atmosphere. We conclude that ikaite dissolution within the water column is responsible for the seawaters' continual pCO_2 undersaturation. In addition, we discuss that dissolution of ikaite crystals exported from sea ice in the underlying seawater can potentially hamper the effect of oceanic acidification on $\Omega_{aragonite}$ in fall and winter in ice-covered areas at the time when $\Omega_{aragonite}$ is smallest.

7. Acknowledgments

8. References

Bates, N. R., Cai, W. J., and Mathis, J. T.: The ocean carbon cycle in the western Arctic Ocean: Distributions and air-sea fluxes of carbon dioxide, Oceanography, 24, 186-201, 2011.

Bates, N. R. and Mathis, J. T.: The Arctic Ocean marine carbon cycle: evaluation of air-sea CO_2 exchanges, ocean acidification impacts and potential feedbacks, Biogeosciences, 6, 2433-2459, 2009.

Bates, N. R., Garley, R., Frey, K. E., Shake, K. L., Mathis, J. L.: Sea-ice melt CO_2-carbonate chemistry in the western Arctic Ocean: meltwater contribution to air-sea CO_2 gas exchange, mixed-layer properties and rates of net community production under sea ice, Biogeosciences, 11, 6769-6789, doi:10.5194/bg-11-6769-2014, 2014.

592   Chierici, M. and Fransson, A.: Calcium carbonate saturation in the surface water of the Arctic Ocean:

593   undersaturation in freshwater influenced shelves, Biogeosciences, 6, 2421-2431, 2009.

594   Chierici, M., Fransson, A., Lansard, B., Miller, L. A., Mucci, A., Shadwick, E., Thomas, E., Tremblay, J. E. and

595   Papakyriakou, T.: The impact of biogeochemical processes and environmental factors on the calcium carbonate

596   saturation state in the Circumpolar Flaw Lead in the Amundsen Gulf, Arctic Ocean, Journal of Geophysical

597   Research-Oceans, 116, C00G09, doi:10.1029/2011JC007184, 2011.

598   Copin Montégut, C.: A new formula for the effect of temperature on the partial pressure of carbon dioxide in

599   seawater, Marine Chemistry, 25, 29-37, 1988.

600   Cox, G. F. N. and Weeks, W. F.: Equations for determining the gas and brine volumes in sea-ice samples,

601   Journal of Glaciology, 29, 306 - 316, 1983.

602   Delille, B., Vancoppenolle, M., Geilfus, N.-X., Tilbrook, B., Lannuzel, D., Schoemann, V., Becquevort, S.,

603   Carnat, G., Delille, D., Lancelot, C., Chou, L., Dieckmann, G. S., and Tison, J.-L.: Southern Ocean CO_2 sink:

604   The contribution of the sea ice, Journal of Geophysical Research: Oceans, 119, 6340-6355, 2014.

605   Dieckmann, G. S., Nehrke, G., Papadimitriou, S., Gottlicher, J., Steininger, R., Kennedy, H., Wolf-Gladrow, D.,

606   and Thomas, D. N.: Calcium carbonate as ikaite crystals in Antarctic sea ice, Geophysical Research Letters, 35,

607   2008.

608   DOE (Ed.): Handbook of methods for the analysis of the various parameters of the carbon dioxide system in sea

609   water, 1994.

610   Ducklow, H. W.: Seasonal production and bacterial utilization of DOC in the Ross Sea, Antarctica, Biogeochem.

611   Ross Sea, vol 78, 143-158, 2003.

612   Else, B. G. T., Galley, R. J., Lansard, B., Barber, D. G., Brown, K., Miller, L. A., Mucci, A., Papakyriakou, T.

613   N., Tremblay, J. E., and Rysgaard, S.: Further observations of a decreasing atmospheric CO_2 uptake capacity in

614   the Canada Basin (Arctic Ocean) due to sea ice loss, Geophysical Research Letters, 40, 1132-1137, 2013.

615   Else, B. G. T., Papakyriakou, T., Galley, R., Drennan, W. M., Miller, L. A., and Thomas, H.: Wintertime CO_2

616   fluxes in an Arctic polynya using eddy covariance: Evidence for enhanced air-gas transfer during ice formation,

617   Journal of Geophysical Research, 116, 2011.

618   Else, B. G. T., Rysgaard, S., Attard, K., Campbell, K., Crabeck, O., Galley, R. J., Geilfus, N. X., Lemes, M.,

619   Lueck, R., Papakyriakou, T., and Wang, F.: Under-ice eddy covariance flux measurements of heat, salt,

620   momentum, and dissolved oxygen in an artificial sea ice pool, Cold Regions Science and Technology, 119, 158-
621   169, 2015.

622   Frankignoulle, M.: Field-Measurements of Air Sea CO_2 Exchange, Limnology and Oceanography, 33, 313-322,
623   1988.

624   Fransson, A., Chierici, M., Miller L. A., Carnat G., Shadwick, E., Thomas, H., Pineault, S. and Papakyriakou, T.
625   N.: Impact of sea-ice processes on the carbonate system and ocean acidification at the ice-water interface of the
626   Amundsen Gulf, Arctic Ocean, Journal of Geophysical Research: Oceans, 118, 7001-7023, 2013.

627   Galley, R. J., Else, B. G. T., Geilfus, N. X., Hare, A. A., Isleifson, D., Barber, D. G., and Rysgaard, S.: Imaged
628   brine inclusions in young sea ice-Shape, distribution and formation timing, Cold Regions Science and
629   Technology, 111, 39-48, 2015.

630   Garneau, M. E., Vincent, W. F., Alonso-Sáez L., Gratton, Y., Lovejoy, C.:Prokaryotic community structure and
631   heterotrophic production in a river-influenced coastal arctic ecosystem, Aquat. Microb. Ecol., 32, 27-40, 2006.

632   Geilfus, N. X., Carnat, G., Dieckmann, G. S., Halden, N., Nehrke, G., Papakyriakou, T., Tison, J. L., and Delille,
633   B.: First estimates of the contribution of $CaCO_3$ precipitation to the release of CO_2 to the atmosphere during
634   young sea ice growth, Journal of Geophysical Research, 118, 2013a.

635   Geilfus, N. X., Carnat, G., Papakyriakou, T., Tison, J. L., Else, B., Thomas, H., Shadwick, E., and Delille, B.:
636   Dynamics of pCO_2 and related air-ice CO_2 fluxes in the Arctic coastal zone (Amundsen Gulf, Beaufort Sea),
637   Journal of Geophysical Research-Oceans, 117, 2012.

638   Geilfus, N. X., Galley, R. J., Cooper, M., Halden, N., Hare, A., Wang, F., Søgaard, D. H., and Rysgaard, S.:
639   Gypsum crystals observed in experimental and natural sea ice, Geophysical Research Letters, doi:
640   10.1002/2013GL058479, 2013b. 2013GL058479, 2013b.

641   Geilfus, N. X., Galley, R. J., Crabeck, O., Papakyriakou, T., Landy, J., Tison, J. L., and Rysgaard, S.: Inorganic
642   carbon dynamics of melt-pond-covered first-year sea ice in the Canadian Arctic, Biogeosciences, 12, 2047-2061,
643   2015.

644   Geilfus, N. X., Tison, J. L., Ackley, S. F., Galley, R. J., Rysgaard, S., Miller, L. A., and Delille, B.: Sea ice pCO_2
645   dynamics and air-ice CO_2 fluxes during the Sea Ice Mass Balance in the Antarctic (SIMBA) experiment -
646   Bellingshausen Sea, Antarctica, The Cryosphere, 8, 2395-2407, 2014.

647   Golden, K. M., Eicken, H., Heaton, A. L., Miner, J., Pringle, D. J., and Zhu, J.: Thermal evolution of
648   permeability and microstructure in sea ice, Geophysical Research Letters, 34, 2007.

649   Goyet, C. and Poisson, A.: New determination of carbonic acid dissociation constants in seawater as a function
650   of temperature and salinity, Deep-Sea Research Part a-Oceanographic Research Papers, 36, 1635-1654, 1989.

651   Grasshoff, K., Ehrhardt, M., and Kremling, K.: Methods of sea water analysis, Verlag Chemie, 1983. 1983.

652   Hansen, J. W., Thamdrup, B., and Jørgensen, B. B.: Anoxic incubation of sediment in gas-tight plastic bags: a
653   method for biogeochemical processes studies, Marine Ecology-Progress Series, 208, 273-282, 2000.

654   Haraldsson, C., Anderson, L. G., Hassellov, M., Hulth, S., and Olsson, K.: Rapid, high-precision potentiometric
655   titration of alkalinity in ocean and sediment pore waters, Deep sea Research I, 44, 2031-2044, 1997.

656   Hare, A. A., Wang, F., Barber, D., Geilfus, N. X., Galley, R. J., and Rysgaard, S.: pH Evolution in sea ice grown
657   at an outdoor experimental facility, Marine Chemistry, 154, 46-54, 2013.

658   Johnson, K. M., Sieburth, J. M., Williams, P. J. L., and Brandstrom, L.: Coulometric total carbon-dioxide
659   analysis for marine studies – automation and calibration, Marine Chemistry, 21, 117-133, 1987.

660   Killawee, J. A., Fairchild, I. J., Tison, J. L., Janssens, L., and Lorrain, R.: Segregation of solutes and gases in
661   experimental freezing of dilute solutions: Implications for natural glacial systems, Geochimica Et Cosmochimica
662   Acta, 62, 3637-3655, 1998.

663   Kirchmann, D. L.: Leucine incorporation as a measure of biomass production by heterotrophic bacteria.
664   Handbook of Methods in Aquatic Microbial Ecology, Chap. 58, 509-518, 1993.

665   Kirchmann, D. L.: Measuring bacterial biomass production and growth rates from Leucine incorporation in
666   natural aquatic environments. Methods in Microbiology, Chap. 12, 227-237, 2001.

667   Leppäranta, M. and Manninen, T.: The brine and gas content of sea ice with attention to low salinities and high
668   temperatures, Helsinki, 1988.

669   Loose, B., McGillis, W. R., Perovich, D., Zappa, C. J., and Schlosser, P.: A parameter model of gas exchange for
670   the seasonal sea ice zone, Ocean Science, 10, 17-28, 2014.

671   MacGilchrist, G. A., Garabato, A. C. N., Tsubouchi, T., Bacon, S., Torres-Valdes, S., and Azetsu-Scott, K.: The
672   Arctic Ocean carbon sink, Deep-Sea Research Part I-Oceanographic Research Papers, 86, 39-55, 2014.

673 Miller, L. A., Papakyriakou, T., Collins, R. E., Deming, J., Ehn, J., Macdonald, R. W., Mucci, A., Owens, O.,

674 Raudsepp, M., and Sutherland, N.: Carbon Dynamics in Sea Ice: A Winter Flux Time Series, Journal of

675 Geophysical Research-Oceans, 116, 2011.

676 Nomura, D., Eicken, H., Gradinger, R., and Shirasawa, K.: Rapid physically driven inversion of the air-sea ice

677 CO_2 flux in the seasonal landfast ice off Barrow, Alaska after onset surface melt, Continental Shelf Research, 30,

678 1998-2004, 2010.

679 Nomura, D., Granskog, M. A., Assmy, P., Simizu, D., and Hashida, G.: Arctic and Antarctic sea ice acts as a

680 sink for atmospheric CO_2 during periods of snowmelt and surface flooding, Journal of Geophysical Research:

681 Oceans, doi: 10.1002/2013JC009048, 2013. 6511-6524, 2013.

682 Parsons T. R., Maita Y., Lali C. M.: A manual of chemical and biological methods for seawater analysis.

683 Pergamon Press, Toronto, 1984

684 Papadimitriou, S., Kennedy, H., Kattner, G., Dieckmann, G. S., and Thomas, D. N.: Experimental evidence for

685 carbonate precipitation and CO_2 degassing during sea ice formation, Geochimica et Cosmochimica Acta, 68,

686 1749-1761, 2004.

687 Papakyriakou, T. and Miller, L.: Springtime CO_2 exchange over seasonal sea ice in the Canadian Arctic

688 Archipelago, Annals of Glaciology, 52, 2011.

689 Parmentier, F.-J. W., Christensen, T. R., Sørensen, L. L., Rysgaard, S., McGuire, A. D., Miller, P. A., and

690 Walker, D. A.: The impact of lower sea-ice extent on Arctic greenhouse-gas exchange, Nature climate change,

691 doi: DOI:10.1038/NCLIMATE1784, 2013. 195-202, 2013.

692 Pierrot, D., Lewis, E., and Wallace, D. W. R.: MS Excel Program Developed for CO_2 System Calculations,

693 Carbon Dioxide Information Analysis Center, Oak Ridge National Laboratory, U.S. Department of Energy, Oak

694 Ridge, Tennessee, doi: 10.3334/CDIAC/otg.CO2SYS_XLS_CDIAC105a, 2006. ORNL/CDIAC-105a. , 2006.

695 Popova, E. E., Yool, A., Aksenov, Y., Coward, A. C., and Anderson, T. R.: Regional variability of acidification

696 in the Arctic: a sea of contrasts, Biogeosciences, 11, 293-308, 2014.

697 Rysgaard, S., Bendtsen, J., Pedersen, L. T., Ramlov, H., and Glud, R. N.: Increased CO_2 uptake due to sea ice

698 growth and decay in the Nordic Seas, Journal of Geophysical Research, 114, 2009.

699 Rysgaard, S., Glud, R. N., Sejr, M. K., Bendtsen, J., and Christensen, P. B.: Inorganic carbon transport during

700 sea ice growth and decay: A carbon pump in polar seas, Journal of Geophysical Research-Oceans, 112, 2007.

701 Rysgaard, S., Søgaard, D. H., Cooper, M., Pu, cacute, ko, M., Lennert, K., Papakyriakou, T. N., Wang, F.,

702 Geilfus, N. X., Glud, R. N., Ehn, J., McGinnis, D. F., Attard, K., Sievers, J., Deming, J. W., and Barber, D.:

703 Ikaite crystal distribution in winter sea ice and implications for CO_2 system dynamics, The Cryosphere, 7, 707-

704 718, 2013.

705 Rysgaard, S., Wang, F., Galley, R. J., Grimm, R., Notz, D., Lemes, M., Geilfus, N. X., Chaulk, A., Hare, A. A.,

706 Crabeck, O., Else, B. G. T., Campbell, K., Sørensen, L. L., Sievers, J., and Papakyriakou, T.: Temporal

707 dynamics of ikaite in experimental sea ice, The Cryosphere, 8, 1469-1478, 2014.

708 Sabine, C. L., Feely, R. A., Gruber, N., Key, R. M., Lee, K., Bullister, J. L., Wanninkhof, R., Wong, C. S.,

709 Wallace, D. W. R., Tilbrook, B., Millero, F. J., Peng, T. H., Kozyr, A., Ono, T., and Rios, A. F.: The oceanic

710 sink for anthropogenic CO_2, Science, 305, 367-371, 2004.

711 Sejr, M. K., Krause-Jensen, D., Rysgaard, S., Sorensen, L. L., Christensen, P. B., and Glud, R. N.: Air-sea flux

712 of CO_2 in arctic coastal waters influenced by glacial melt water and sea ice, Tellus Series B Chemical and

713 Physical Meteorology, 63, 815-822, 2011.

714 Semiletov, I. P., Makshtas, A., Akasofu, S. I., and Andreas, E. L.: Atmospheric CO_2 balance: The role of Arctic

715 sea ice, Geophysical Research Letters, 31, 2004.

716 Søgaard, D. H., Thomas, D. N, Rysgaard, S., Norman, L., Kaartokallio, H., Juul-Pedersen T., Glud, R. N. and

717 Geilfus, N. X.: The relative contributions of biological and abiotic processes to the carbon dynamics in subarctic

718 sea ice, Polar Biol., doi:10.1007/s00300-013-1396-3, 2013.

719 Yamamoto, A., Kawamiya, M., Ishida, A., Yamanaka, Y., and Watanabe, S.: Impact of rapid sea-ice reduction in

720 the Arctic Ocean on the rate of ocean acidification, Biogeosciences, 9, 2365-2375, 2012.

721 Yamamoto-Kawai, M., McLaughlin, F. A., Carmack, E. C., Nishino, S., and Shimada, K.: Aragonite

722 Undersaturation in the Arctic Ocean: Effects of Ocean Acidification and Sea Ice Melt, Science, 326, 1098-1100,

723 2009.

724 Yamamoto-Kawai, M., McLaughlin, F. A., Carmack, E. C., Nishino, S., and Shimada, K.: Freshwater budget of

725 the Canada Basin, Arctic Ocean, from salinity, delta O-18, and nutrients, Journal of Geophysical Research-

726 Oceans, 113, 12, 2008.

727 Zeebe, R. E. and Wolf-Gladrow, D.: CO_2 in seawater: Equilibrium, Kinetics, Isotopes, Elsevier, 2001. 2001.

728

729   **9. Table**

730   Table 1: Seawater conditions on 11 January, before any sea ice formation (t=0), on 25 January, just

731   before the heat was turned back on and on 29 January, at the end of the experiment. Note

732   that seawater salinity and $TA_{(sw)}$ do not reach the initial seawater values as sea ice was still

733   present at the end of the experiment.

Date	Temperature (°C)	Salinity	TA (µmol kg⁻¹)	nTA (µmol kg⁻¹)	TCO₂ (µmol kg⁻¹)	nTCO₂ (µmol kg⁻¹)
11 Jan.	-1.4	33.5	2453	2416	2341	2306
25 Jan.	-1.9	35.5	2659	2471	2524	2346
29 Jan.	-0.6	34.4	2607	2500	2461	2361

734

735

Table 2: Masses of TCO_2 in the water column ($TCO_{2(sw)}$) and in the ice cover ($TCO_{2(ice)}$), masses of ikaite within the ice cover estimated from this study and from Rysgaard et al., (2014), masses of ikaite dissolved in the water column (Ikaite$_{(sw)}$) and masses of CO_2 exchanged between the ice and the atmosphere over the whole pool (estimation based on the air-ice CO_2 fluxes). All units are in mole.

January (DOY)	$TCO_{2(sw)}$	$TCO_{2(ice)}$	Ikaite$_{(ice)}$ from this study	Ikaite$_{(ice)}$ from Rysgaard et al., (2014)	Ikaite$_{(sw)}$	$CO_{2(air-ice)}$
t=0	1041					
13.75	1040	2.38	0.17	0.00	0.47	
13.88	1044	2.09	0.00	0.00	0.87	
14	1043	2.90	0.25	0.00	0.83	0.03
14.13	1043	3.29	0.62	0.00	2.57	0.02
14.25	1038	4.91	-0.05	0.00	1.06	0.01
14.5	1037	4.77	0.18	0.00	3.75	0.12
14.75	1039	4.36	0.12	0.05	2.73	0.07
15	1037				1.80	0.08
15.25	1032	4.67	0.98	0.68	1.28	0.01
15.5	1034	3.89	1.58	0.00	-1.57	0.07
15.92	1034	4.47	0.69	0.00	1.63	0.12
16.38	1024	7.36	1.45	0.08	3.60	0.19
16.67	1028	8.17	1.87	0.00	6.00	0.10
17.38	1023	15.48	0.29	0.65	3.90	0.22
17.67	1026	13.26	0.04	0.46	4.50	0.13
18.38	1030	11.39	0.74	2.14	5.61	0.38
18.67	1027	12.06	0.21	0.21	7.16	0.10
19.38	1029	11.13	0.01	0.84	6.96	0.23
19.67	1030	10.75	0.03	0.09	1.97	0.11
20.38	1028	10.25	-0.12	0.23	1.47	0.42
20.67	1022	10.36	-0.70	0.71	3.48	0.12
21.38	1025	10.50	0.88	0.35	7.42	0.35
23.63	1034	12.60	1.34	2.14	11.18	
24.38	1026	14.84	1.30	1.94	9.75	0.21
25.38	1017	15.67	1.09	3.05	6.62	
25.5	1029				11.51	0.02
28.67	1022	13.46	-0.57	0.46	20.91	-0.93
29.38	987.3	15.82	-0.56	0.55	26.72	-0.15